Response to Reviewer #2

Overall impression

The manuscript analyzed the biochemical influences of mesoscale eddies (including normal and abnormal eddies) in the Southern Ocean, by using machine learning and multi-source marine dataset. The manuscript estimated chlorophyll (Chl) and dissolved inorganic carbon (DIC) contributions to pCO_2, and found their seasonal variations. These results are interesting and are of vital importance on global biogeochemical cycles and the climate change. However, some description about methods/data are ambiguous and few conclusions need to be further discussed.

Response: We would like to thank reviewer 2 for taking the time to review the manuscript and for its valuable feedback. We acknowledge that the suggestions provided have really helped to improve the quality of this work. We hope the answers and information provided here would respond to what was demanded.

Major questions:

1. There are some other methods to identify abnormal eddies, such as using potential density and directions of geostrophic current. They are supposed to be introduced in the introduction, and point out why authors choose the method of SSTA.

Response: We acknowledge that there are other methods to identify abnormal eddies, such as using potential density and geostrophic current direction (Mcgillicuddy, 2015). We have added this information in the introduction. We also clarified why we chose to use SSTA to distinguish between normal and abnormal eddies. Recent studies have found that abnormal eddies show opposite SSTA signals to normal eddies (Leyba et al., 2017; Liu et al., 2020; Liu et al., 2021; Ni et al., 2021). Compared to potential density, SSTA data can be obtained from satellite remote sensing with higher spatial and temporal resolutions, making it a convenient and reliable data source for identifying eddies (Castellani, 2006; Liu et al., 2021).

Moreover, detecting eddies using directions of geostrophic current is essentially based on SSH features. Our study utilizes the abnormal eddy dataset that Liu et al. (2021) developed, which uses a deep learning model to fuse satellite SSH and SST data. The method can simultaneously extract SSH features for determining eddy locations and extract SST information to help distinguish between normal and abnormal eddies with great accuracy and efficiency. In addition, the method is able to detect eddies in regions where traditional methods may not be effective, such as in regions with weak eddies or regions with complex oceanic dynamics (Liu et al., 2021). Given its high accuracy and comprehensive information on eddy characteristics, we find this dataset to be particularly useful for our study.

2. The methods to derive pCO_2 from Chl, SST, DIC and other variables are supposed to be introduced with more descriptions or equations.

Response: We have added the following details to explicitly describe the methods to derive pCO_2:

" The pCO_2 field is calculated from TA, DIC, SST, and SSS based on seawater CO_2 chemistry (Iida et al., 2021). Firstly, the mean rates of regional pCO_2 and multiple regressions are used to derive the algorithms of pCO_2 expressed empirically as a function of in situ TA, DIC, SST, SSS, and the year. Then, the pCO_2 fields that filled both in space (1° × 1°) and time (monthly) are drawn by applying global data sets of TA, DIC, SST, and SSS to the variables in these empirical equations."

3. The method to define and identify abnormal eddies should be introduced in detail even if the authors cited the paper of Liu et al., 2021. Did they identify abnormal eddies according to SSTA>0/SSTA<0 within eddy boundaries/cores? How did they distinguish AEs and CEs just according to SSTA?

Response: We have updated the manuscript to include more detailed information on our methodology for identifying abnormal eddies. We distinguish between normal and abnormal eddies based on the mean SSTA within eddy boundaries. Besides, we distinguish between AEs and CEs based on the SSHA, as AEs (CEs) are usually accompanied by local convergence (divergence), leading to positive (negative) SSHA. Therefore, WAEs are identified according to SSHA >0 and SSTA >0, CAEs are identified according to SSHA >0 and SSTA <0, CCEs are identified according to SSHA <0 and SSTA <0, and WCEs are identified according to SSHA <0 and SSTA >0.

4. The descriptions about eddy dataset and identification are very poor. In line 139, the authors mentioned "the ground truth data set". What's the ground truth data set of eddies? Is it produced by the authors or a public dataset? That's important to the verification.

Response: We have verified in the manuscript that the ground truth dataset of mesoscale eddies used in our study was generated automatically using the SSH-based method proposed by Haller (2005), and the eddy dataset was produced by Liu et al. (2021).

5. How did authors match daily eddy dataset with monthly DIC and pCO_2 temporally and spatially when doing composite analyses? Temporally, is eddy at JAN. 31st matched with DIC of JAN. or Feb. data? is DIC data used within eddy boundaries or eddy cores?

Response: We have added a schematic in the Supporting Information and revised the section to provide additional details on the methodology used to create the composite

eddies. The positions of co-located SST, Chl-*a*, DIC, and pCO_2 observations are normalized by R, which defines the edge of an eddy as ±1 and the eddy core as 0. This allowed us to construct composite averages from eddies of varying sizes. We then extract data from −2R to 2R to include the interactions between eddies and the surrounding waters and interpolate them onto an evenly spaced 17 by 17 grid to create the surface composite patterns. Therefore, the mean anomalies of SST, Chl-*a*, DIC, and pCO_2 are used within eddy boundaries. For daily SST and Chl-*a*, we perform the eddy-centric composite method matching eddies and variables on the same day and calculate the mean value, as shown in the following Fig. 1a. By contrast, for monthly DIC and pCO_2, we calculate the eddy-centric composite maps, using all eddies of the same month with DIC and pCO_2 of that month and calculate the mean value (Fig. 1b below).

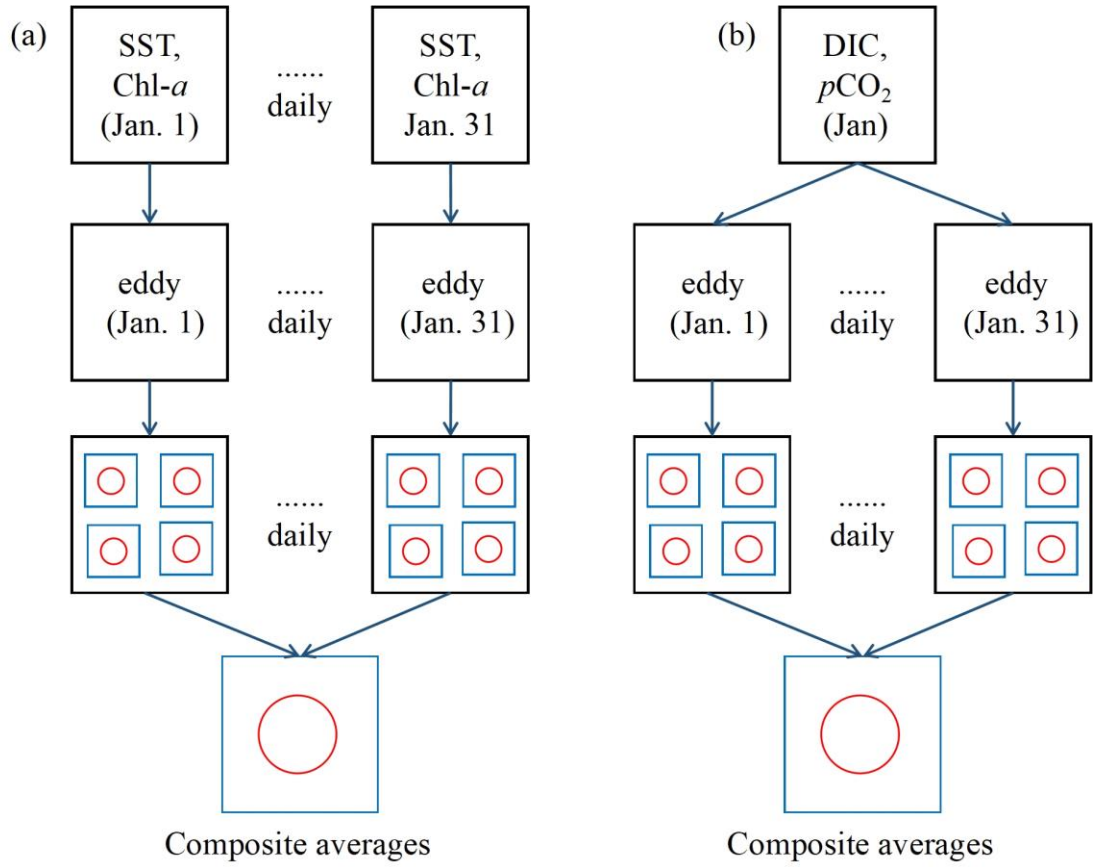

Figure 1. Schematic of eddy-centric composite method for daily (a) SST and Chl-*a* and monthly (b) DIC and pCO_2, taking January as an example.

6. Taking CEs for example, commonly, upwellings are thought to transport cold water to the sea surface, as well as richer nutrients at the same time. Therefore, CEs often show lower SST and higher chlorophyll. The conclusions from Figure 8 show SSTA within abnormal eddies are dominant by Ekman pumping. However, the chlorophyll anomalies of abnormal eddies are attributed to eddy pumping. The conclusions are contradictory to each other. If they are reliable, what's the mechanism leading to contrasting vertical process on SST and chlorophyll respectively? Therefore, discussions of lines 279-280 and 295-296 need more explanations. Besides, line 279 should be "eddy-induced Ekman pumping".

Response: We have revised the manuscript accordingly and deepened the discussion. In response to the question, we further calculated the mean gradient of SST and Chl-*a*, which are normalized prior to calculation. The average gradients of SST and Chl-*a* are found to be 0.05 and 0.11, respectively. The north-south gradients (north is the positive direction) of SST and Chl-*a* are 0.04 and −0.02, respectively. The east-west gradients (east is the positive direction) of SST and Chl-*a* are 0.00 and −0.04, respectively. As eddy stirring redistribute physical and biogeochemical parameters spatially through horizontal advection, the larger the horizontal parameter gradient, the stronger the eddy stirring effect (Mcgillicuddy, 2016). The small gradient of SST leads to a negligible effect of eddy stirring. Within abnormal eddies, the effect of eddy-induced pumping overcomes the effect of eddy pumping, resulting in the opposite SST anomalies in normal and abnormal eddies.

Compared to SST, Chl-*a* has a higher gradient, resulting in a stronger effect of eddy stirring. The gradients of Chl-*a* suggest that the climatological Chl-*a* increases southward and westward. Counterclockwise rotation of AEs in the SO would advect low Chl-*a* from the northeast to the west and high Chl-*a* from the southwest to the east. The reverse is true for CEs. Previous works found that the dipole shapes arising from stirring tend to be asymmetric, with larger anomalies at the leading compared to the trailing side of eddies (Chelton et al., 2011; Frenger et al., 2015; Dawson et al., 2018; Frenger et al., 2018). As the major propagation direction of eddies is westward, the composite Chl-*a* anomalies in AEs/CEs show dominant negative/positive signals due to eddy stirring. Besides, eddy pumping tends to produce Chl-*a* anomalies of the same sign. The common effects of eddy stirring and eddy pumping overcome the effect of eddy-induced Ekman pumping, resulting in similar patterns of Chl-*a* anomalies in normal and abnormal eddies.

However, from Figs. 8b1–b4 and f1–f4 in the manuscript, we can see that the magnitudes of Chl-*a* anomalies within normal eddies are higher than abnormal eddies, which reflects the effect of eddy-induced Ekman pumping. Besides, in some regions with small amplitude, such as the south of ACC and the South Pacific Ocean, we find Chl-*a* anomalies in AEs/CEs are positive/negative (Figs. 6e–h in the manuscript). Such a result may be caused by a more dominant effect of eddy-induced Ekman pumping on Chl-*a*. Overall, eddy stirring and eddy pumping are mainly responsible for the patterns of Chl-*a* anomalies within eddies in the SO, and eddy-induced Ekman pumping attenuates the magnitudes of Chl-*a* anomalies within abnormal eddies.

7. The manuscript is supposed to evaluate the accuracies of abnormal eddy identification method, which can combine with Argo profiles via temperature and potential density. At the same time, it should point out the method improvement in future

Response: We have updated the manuscript to reflect these points. The experiments

showed that the model could accurately identify abnormal eddies in the South China Sea (SCS) and Kuroshio Extension (KE) region (Liu et al., 2021). In addition, Argo floats data also verified the accuracy and validity of the model (Liu et al., 2021). However, we also acknowledge that there is room for improvement in our method. Considering that the changes in SSH, SST, Chl-*a*, and roughness caused by eddies can be recorded by altimeter, infrared, ocean color, and synthetic aperture radar (SAR) remote sensing, respectively. Besides, potential density and temperature recorded by Argo floats can also identify abnormal eddies. In future work, we will combine multiple remote sensing data with Argo profiles to evaluate the accuracies of abnormal eddy identification method.

Minor questions:

1. Lines 31-32: Authors point out that eddies have influences on "biochemical parameters". While, the listed references are both about chlorophyll, which is a biological parameter. References about chemical parameters should be introduced.

Response: References about chemical parameters have been added.

2. Lines 37-39: Rotations of eddies are related to the hemisphere. It should illustrate which hemisphere is talked about.

Response: When mentioning the rotations of the eddies, we emphasized that the eddies is in the Southern Hemisphere.

3. Line 56: How about eddy influence on chlorophyll during wintertime with deeper mixing?

Response: We have added information and references about the influence of eddies on Chl-*a* during wintertime with deeper mixing in the introduction. Dufois et al. (2014) suggested that deeper mixed layers could explain long-lived Chl-*a* anomalies in anticyclones of the South Indian Ocean between 20°S and 30°S. Both mixing and eddy-induced Ekman pumping tend to produce Chl-*a* anomalies of the same sign. For instance, shallower mixed layers in cyclonic eddies could result in higher Chl-*a*, while deeper mixed layers in anticyclonic eddies could lead to lower Chl-*a*.

In our study, eddy stirring and eddy pumping are the main modulation processes of normal and abnormal eddies to Chl-*a* in the SO. Composite Chl-*a* anomalies display negative signatures in both WAEs and CAEs and positive signatures in CCEs and WCEs. Therefore, we do not specifically address the influence of eddies on Chl-*a* during wintertime with deeper mixing in our study.

4. Lines 107-108: The expression of OI-SST should be in agreement.

Response: We have corrected the expression of OI-SST.

5. Line 166: JMA is suggested to be introduced as Japan Meteorological Agency.

Response: We have introduced JMA as "Japan Meteorological Agency" upon its first mention in the manuscript.

6. Line 178: What are the denominators when calculating eddy frequencies? It should be expressed more clearly.

Response: We have added the definition of eddy frequency. The eddy frequency is the ratio of the number of days eddies appeared to the total number of observation days.

7. Lines 186-187: The conclusion is true in South America, but not evident in the south of Australia.

Response: We have revised the manuscript to demonstrate the findings explicitly. Based on Figs. 4c and 4f in the manuscript, it can be observed that abnormal eddies have a polarity distribution opposite to that of normal eddies in the continental boundary currents where more CCEs and CAEs occur. However, it should be noted that more WAEs and WCEs occur in the south of Australia.

8. Line 285: How to understand "eddy trapping has little influence on Chl-*a*"? Please give more descriptions to explain it.

Response: We have added more descriptions to explain why eddy trapping has little influence on Chl-*a*. Nonlinear eddies tend to trap the fluid contained in their interiors (Provenzale, 1999; Mcgillicuddy, 2016). The composition of the trapped fluid is dependent on various factors, including the eddy propagation and the local gradients in physical and biochemical properties. The tracks of long-lived eddies with lifetimes longer than 1 year show that the major propagation direction of eddies is westward, with AEs propagating north and CEs propagating south. Due to the climatological Chl-*a* increasing southward, AEs propagating northward tend to trap high Chl-*a* into northern areas with low Chl-*a*, as shown in Fig. 2 below. On the other hand, CEs propagating southward tend to trap low Chl-*a* into southern areas with high Chl-*a*. Such effect of eddy trapping on Chl-*a* contradicts the actual composite Chl-*a* anomalies over eddies with negative Chl-*a* anomalies in AEs and positive Chl-*a* anomalies in CEs. As a result, we conclude that eddy trapping has little influence on Chl-*a*.

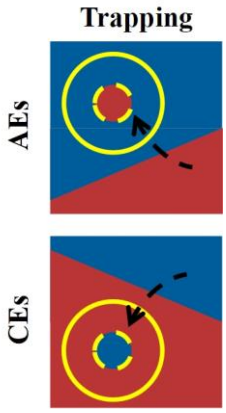

Figure 2. Schematic illustrating the eddy trapping of how AEs and CEs affect Chl-*a*. Red and blue colors represent high and low Chl-*a*, respectively.

9. Lines 303-314: Are those conclusions for summertime still "dominant"? The magnitudes seem similar for summertime.

Response: Yes, there are no significant seasonal variations in eddy-induced SST, Chl-*a*, and DIC anomalies. Therefore, the dominant mechanisms of eddies affecting these variables do not alter by season.

10. Figure 11 is suggested to be shown in wintertime and summer time respectively, based on which Figure 8, Figure 12, and Figure 13 can be better discussed.

Response: We appreciate the suggestion, but given the nature of our findings, we feel that presenting the annual mean is more appropriate for our study. In the original manuscript, we did not discuss the SST, Chl-*a*, and DIC anomalies within the eddies seasonally, as their variations did not exhibit significant seasonal patterns. Therefore, we opted to present the annual mean eddy-induced Ekman pumping in Figure 11, as it provides a comprehensive representation of the differences in variable anomalies between normal and abnormal eddies. We believe that this approach allows for a more convenient and meaningful comparison of the variable anomalies within the eddies.

11. In Figure 4, lines 558-599, the authors mean blue and red colors in the right column. However, blue and red colors are shown in each sub-figure, which is misleading.

Response: We have revised the manuscript to ensure that the blue and red colors are clearly associated with the right column only.

12. Figures 4d and 4e show that abnormal eddies occur along fronts, where eddies are active, and along offshore areas where accuracies of altimeters are low. It is suggested to show ratios of abnormal eddies to normal eddies (WAEs/CAEs, CCEs/WCEs). Will the abnormal eddy signals offshore be amplified offshore? What are the mean depths of clustered abnormal eddies? It should be cautious with eddies shallower than 1000 m.

Response: We appreciate the reviewer's insightful suggestions, and we calculated the ratios of abnormal eddies to normal eddies, as shown in Fig. 3 below. We find more CAEs in the Western Boundary Current (WBC) regions and significant dominance of WCEs in southern Australia. In the southeast of America and Campbell Plateau, with depths shallower than 1000 m (Fig. 4 below), abnormal eddy signals offshore may be amplified offshore due to the low accuracies of altimeters along offshore areas. We further calculate the mean depths of clustered eddies. The mean depths of WAEs, CAEs, CCEs, and WCEs are 4086 m, 3969 m, 4044 m, and 4014 m. All of them are deeper than 1000m. As mentioned in the manuscript, eddies disappear in regions shallower than 2000m because the bottom topography constrains the generation of eddies. Therefore, the amplified abnormal eddy signals in the southeast of America and Campbell Plateau have little influence on the results.

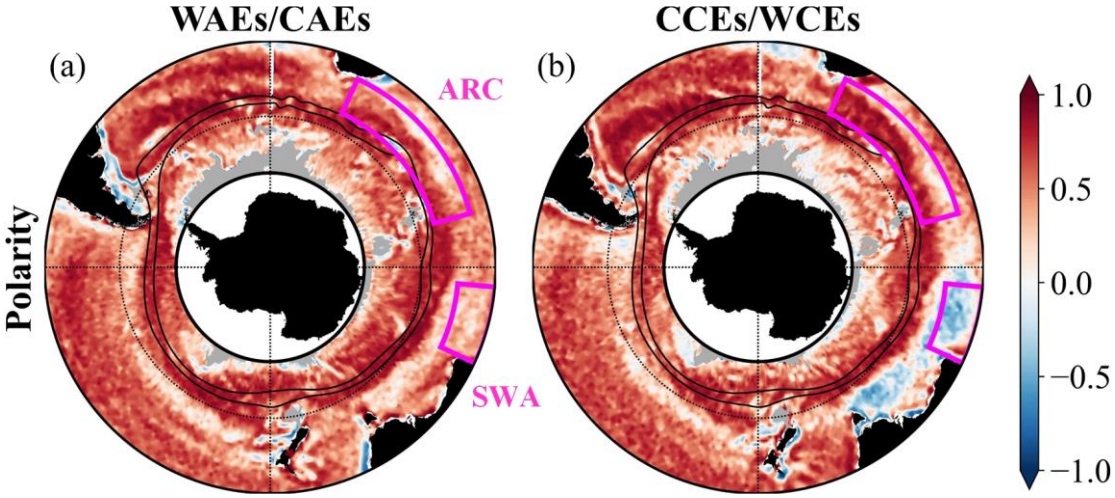

Figure 3. Spatial distribution of eddy polarity dominance in the SO from 1996 to 2015. (a) Ratio of the area occupied by WAEs over the area covered by CAEs. (b) Ratio of the area occupied by CCEs over WCEs. Values >0 in red and <0 in blue mark the dominance of normal and abnormal eddies, respectively. Black solid lines show the mean northern and southern positions of the ACC major fronts. The black dotted circle is 50° S. The magenta boxes represent ARC and SWA regions.

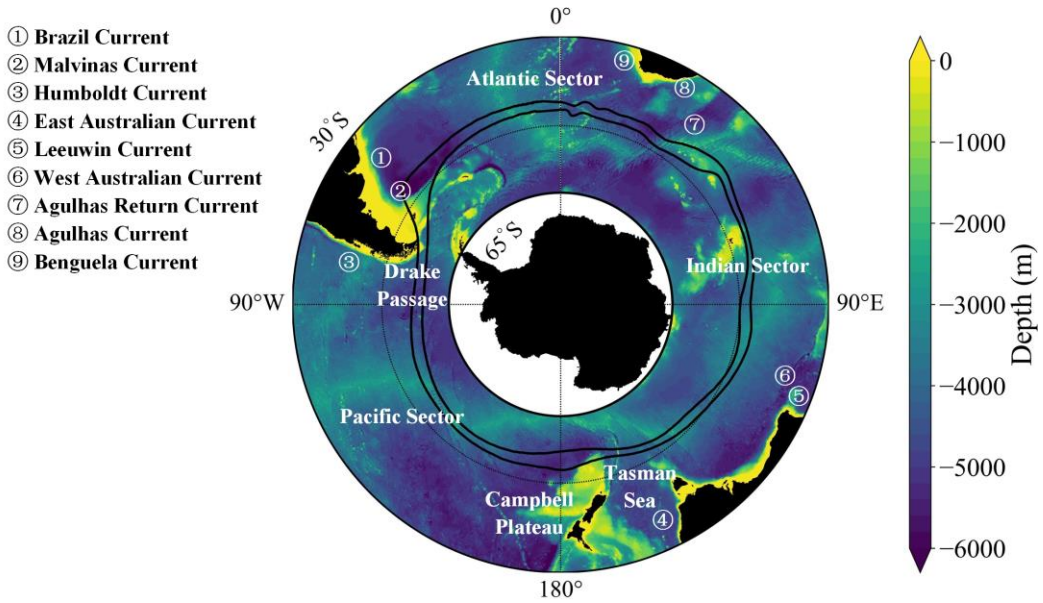

Figure 4. Southern Ocean topography and current. Black solid lines show the mean northern and southern positions of the ACC major fronts. The black dotted circle is 50° S.

13. Figure 6. The abnormal eddies are identified from SST so the SSTA of Figure 6 is regular. The other three parameters are very noisy. The magnitudes of chlorophyll and pCO_2 signals induced by abnormal eddies are even higher than normal eddies, which are contrasting with eddy amplitude comparisons. Why?

Response: We have added some explanations to the manuscript to address the reviewer's concern. The distributions of Chl-*a* anomalies over both normal and abnormal eddies are similar to the eddy amplitude distributions, with stronger negative/positive anomalies within AEs/CEs in regions of higher amplitude. This result indicates the dominant effect of eddy pumping on Chl-*a*. However, in regions of lower amplitude, we find the patterns of Chl-*a* anomalies are spotty, with average positive/negative Chl-*a* anomalies in AEs/CEs. Such a result may be caused by a more dominant effect of eddy-induced Ekman pumping on Chl-*a*.

The magnitudes of Chl-*a* anomalies induced by abnormal eddies are even higher than normal eddies in these regions due to the smaller amplitude and eddy pumping of abnormal eddies than normal eddies. Furthermore, in some regions, such as SWA, the magnitudes of pCO_2 anomalies induced by abnormal eddies are higher than normal eddies, which are related to the stronger eddy-induced Ekman pumping of abnormal eddies.

Reference

Castellani, M.: Identification of eddies from sea surface temperature maps with neural

networks, Int. J. Remote Sens., 27, 1601-1618, https://doi.org/10.1080/01431160500462170, 2006.
Chelton, D. B., Gaube, P., Schlax, M. G., Early, J. J., and Samelson, R. M.: The Influence of Nonlinear Mesoscale Eddies on Near-Surface Oceanic Chlorophyll, Science, 334, 328-332, https://doi.org/doi:10.1126/science.1208897, 2011.
Dawson, H. R. S., Strutton, P. G., and Gaube, P.: The Unusual Surface Chlorophyll Signatures of Southern Ocean Eddies, J. Geophys. Res.-Oceans, 123, 6053-6069, https://doi.org/10.1029/2017JC013628, 2018.
Dufois, F., Hardman-Mountford, N. J., Greenwood, J., Richardson, A. J., Feng, M., Herbette, S., and Matear, R.: Impact of eddies on surface chlorophyll in the South Indian Ocean, J. Geophys. Res.-Oceans, 119, 8061-8077, https://doi.org/https://doi.org/10.1002/2014JC010164, 2014.
Frenger, I., Münnich, M., and Gruber, N.: Imprint of Southern Ocean mesoscale eddies on chlorophyll, Biogeosciences, 15, 4781-4798, https://doi.org/10.5194/bg-15-4781-2018, 2018.
Frenger, I., Münnich, M., Gruber, N., and Knutti, R.: Southern Ocean eddy phenomenology, J. Geophys. Res.-Oceans, 120, 7413-7449, https://doi.org/10.1002/2015jc011047, 2015.
Haller, G.: An objective definition of a vortex, J. Fluid Mech., 525, 1-26, https://doi.org/10.1017/S0022112004002526, 2005.
Iida, Y., Takatani, Y., Kojima, A., and Ishii, M.: Global trends of ocean CO2 sink and ocean acidification: an observation-based reconstruction of surface ocean inorganic carbon variables, J. Oceanogr., 77, 323-358, https://doi.org/10.1007/s10872-020-00571-5, 2021.
Leyba, I. M., Saraceno, M., and Solman, S. A.: Air-sea heat fluxes associated to mesoscale eddies in the Southwestern Atlantic Ocean and their dependence on different regional conditions, Clim. Dyn., 49, 2491-2501, https://doi.org/10.1007/s00382-016-3460-5, 2017.
Liu, Y., Yu, L., and Chen, G.: Characterization of Sea Surface Temperature and Air‐Sea Heat Flux Anomalies Associated With Mesoscale Eddies in the South China Sea, J. Geophys. Res.-Oceans, 125, https://doi.org/10.1029/2019jc015470, 2020.
Liu, Y., Zheng, Q., and Li, X.: Characteristics of Global Ocean Abnormal Mesoscale Eddies Derived From the Fusion of Sea Surface Height and Temperature Data by Deep Learning, Geophys. Res. Lett., 48, https://doi.org/10.1029/2021gl094772, 2021.
McGillicuddy, D. J.: Formation of Intrathermocline Lenses by Eddy–Wind Interaction, J. Phys. Oceanogr., 45, 606-612, https://doi.org/10.1175/jpo-d-14-0221.1, 2015.
McGillicuddy, D. J.: Mechanisms of Physical-Biological-Biogeochemical Interaction at the Oceanic Mesoscale, Annu. Rev. Mar. Science, 8, 125-159, https://doi.org/10.1146/annurev-marine-010814-015606, 2016.
Ni, Q., Zhai, X., Jiang, X., and Chen, D.: Abundant Cold Anticyclonic Eddies and Warm Cyclonic Eddies in the Global Ocean, J. Phys. Oceanogr., 51, 2793-2806, https://doi.org/10.1175/jpo-d-21-0010.1, 2021.
Provenzale, A.: TRANSPORT BY COHERENT BAROTROPIC VORTICES, Annu. Rev. Fluid Mech., 31, 55-93, https://doi.org/10.1146/annurev.fluid.31.1.55, 1999.